

Two-Phase Thermal Switch for Lunar Lander and Rover Thermal Management

Nathan Van Velson¹, Jeffrey Diebold², David-Paul Schulze³, Calin Tarau⁴, and William G. Anderson⁵
Advanced Cooling Technologies, Inc., Lancaster, PA, 17601

The 14-earth day long lunar night poses a significant challenge to the thermal management of future lunar landers and rovers. For these vehicles to operate for long durations on the lunar surface, the on-board electronics must be maintained above their survival temperatures during the lunar night. Thermal switches are among the passive thermal management technologies that may be utilized for helping lunar vehicles survive the lunar night while minimizing the use of electric power for survival heating. In this work, a passive thermal switch design with high turndown is developed for lunar landers and rovers. This thermal switch design utilizes a sealed flexible bellows containing a two-phase working fluid. The switching mechanism is passively actuated by the temperature of the heat source. A coupled thermal-mechanical model has been developed to illustrate the dynamic performance of the two-phase thermal switch. Several thermal switch prototypes were fabricated and tested for concept demonstration and model validation, and trade studies for enhancing the ON/OFF conductance ratio were performed. Finally, a design concept for a small lunar rover thermal management system based on the two-phase thermal switch was developed.

Nomenclature

ACT	=	Advanced Cooling Technologies, Inc.
C_x	=	lumped capacitance of thermal mass x
b	=	bellows damping coefficient
F	=	effective force
G_{off}	=	off thermal conductance
K	=	bellows spring rate
M	=	bellows effective mass
NCG	=	non-condensable gas
R_z	=	thermal resistance of thermal link z
TIM	=	thermal interface material
y	=	bellows displacement

I. Introduction

The lunar night poses a significant challenge to the thermal management of lunar landers and rovers. In order for lunar landers and rovers to operate for long durations on the lunar surface, the on-board electronics must be maintained above their survival temperature during the long lunar night. This could be done with the use of survival electric heaters; however, it has been estimated that for every Watt of power supplied by batteries during the lunar night, an additional 5 kg of battery mass is required. Surviving the lunar night without the use of electric power can be enabled by advanced passive thermal management technologies.

Thermal switches are among the passive thermal control devices that can be utilized in lunar lander and rover thermal management systems. Thermal switches are designed to minimize heat transport when in the “Off” condition,

¹ Lead Engineer, Research and Development, 1046 New Holland Ave, Lancaster, PA.

² Engineer III, Research and Development, 1046 New Holland Ave, Lancaster, PA.

³ Engineer I, Research and Development, 1046 New Holland Ave, Lancaster, PA.

⁴ Principal Engineer, Research and Development, 1046 New Holland Ave, Lancaster, PA.

⁵ Chief Engineer, Research and Development, 1046 New Holland Ave, Lancaster, PA.

and to maximize heat transfer when in the “On” condition. The actuation of the thermal switch often happens at a specified set point temperature. To date, most passive thermal switches use the expansion/contraction of a volume to make/break a mechanical contact between two surfaces (Ref. 1-3). These thermal switches typically have a capacity of only a few Watts.

As an alternative, a new passive thermal switch design concept is being developed, capable of transferring higher powers with a high On/Off thermal conductance ratio. This thermal switch design utilizes a sealed flexible bellows that contains a saturated two-phase working fluid. The actuation of the thermal switch is driven by the saturation temperature and pressure of the fluid within the bellows. In this paper, the principles of operation of the two-phase thermal switch are described, and coupled thermal-mechanical model for understanding the dynamic and thermal performance of the thermal switch is presented. Two thermal switch prototype devices were fabricated and tested for concept demonstration. Finally, a thermal switch design concept for a small lunar rover is described.

II. Two-Phase Thermal Switch Design and Operation

A. Thermal Switch Operation

The concept of the two-phase thermal switch is shown in Figure 1. It consists of a hermetically sealed metal bellows which contains a saturated two-phase working fluid. The exterior of the bellows may either be encapsulated in an enclosure, or exposed to ambient. One end of the bellows is fixed to a heat source; the other end is free to move axially. The movement of the bellows end cap is dictated by the balance between the external pressure, the internal vapor pressure, and the restoring force of the bellows. Opposite the free end of the bellows is a heat sink. When the heat source temperature is low, the corresponding saturation temperature and pressure within the bellows is also low, and the bellows is not in contact with the heat sink. As the heat source temperature increases, the vapor pressure within the bellows increases, causing the bellows to expand until it comes in contact with the heat sink, allowing heat to be transferred through the bellows, by evaporation and condensation of the working fluid. The actuation temperature at which the bellows comes into contact with the heat sink is determined by the balance of forces between the vapor pressure of the working fluid and the spring force of the bellows, as well as the pressure of any external gas surrounding the bellows. An internal wick structure can be incorporated for fluid management as well as to enable gravity- and orientation-independent operation.

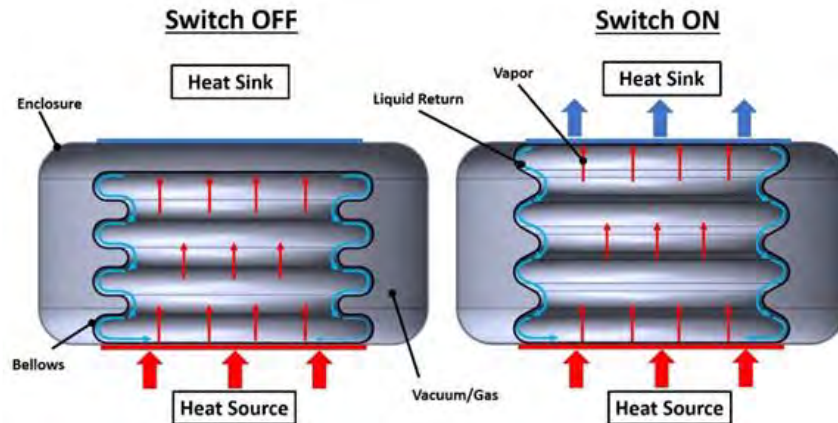


Figure 1: Two-Phase Thermal Switch principle of operation.

B. Thermal Switch Thermal-Mechanical Model

A coupled thermal and structural model for the two-phase thermal switch was developed based on a lumped thermal resistance and capacitance model. The equivalent thermal resistance and capacitance network is shown in Figure 2. An energy balance is taken on each lumped capacitance, for example the bottom bellows end cap A , with capacitance C_A [J/K], which is in thermal contact with the heat source, the top of the enclosure (B) through the enclosure wall, and the bellows interior (C), through specified thermal resistances, R_{th} [K/W]. The heat transfer between two thermal masses is related as $Q = \Delta T/R_{th}$. This leads to a set of ordinary differential equations describing the temperature change of each thermal mass, as shown below:

$$\frac{dT_A}{dt} = \frac{1}{C_A} \left[\dot{Q}_{in} - \frac{T_A - T_B}{R_2} - \frac{T_A - T_C}{R_3} \right] = \frac{1}{C_A} \left[\frac{T_{source} - T_A}{R_1} - \frac{T_A - T_B}{R_2} - \frac{T_A - T_C}{R_3} \right]; \quad (1)$$

$$\frac{dT_B}{dt} = \frac{1}{C_B} \left[\frac{T_A - T_B}{R_2} + \frac{T_D - T_B}{R_5} - \frac{T_B - T_{sink}}{R_6} \right]; \quad (2)$$

$$\frac{dT_C}{dt} = \frac{1}{C_C} \left[\frac{T_A - T_C}{R_3} + \frac{T_C - T_D}{R_4} \right]; \quad (3)$$

$$\frac{dT_D}{dt} = \frac{1}{C_D} \left[\frac{T_C - T_D}{R_4} - \frac{T_D - T_B}{R_5} \right]. \quad (4)$$

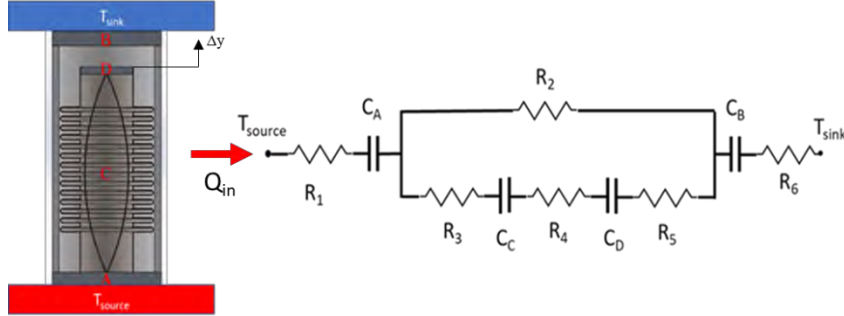


Figure 2: Two-phase thermal switch approximated as a lumped thermal capacitance and resistance model

Each thermal resistance and capacitance can be estimated from the material properties and geometry of the thermal switch design. The boundary conditions for the thermal model are a heat input at the heat source, and the heat sink temperature. The above ordinary differential equations can be solved simultaneously for a given initial temperature distribution and heat source power and heat sink temperature time profile, to obtain the temperatures of each thermal mass and the heat source, as well as the heat transfer between each thermal mass.

In addition to the transient thermal model, a dynamic mechanical model of the bellows is incorporated. The bellows can be approximated as a mass-spring-damper system, with a bellows spring constant k , an effective mass M , and a damping coefficient b . The displacement y of the bellows can be found from the standard mass-spring equation:

$$M\ddot{y} + b\dot{y} + ky = F(t) \quad (5)$$

The forcing term $F(t)$ is the balance of the internal and external pressures on the bellows end cap, and is a function of the saturated vapor temperature in the bellows and the pressure of the NCG in the enclosure.

$$F(t) = F_{NCG} + F_{contact} - F_{saturation} \quad (6)$$

The bellows is not allowed to expand indefinitely; the expansion of the bellows is restricted by contact with the top of the enclosure. When the bellows is in contact with the enclosure, the force from the enclosure gas goes to zero, and a reaction contact force $F_{contact}$ appears, which is equal to the force due to the saturation pressure in the bellows.

III. Thermal Switch Prototype Demonstration

Two thermal switch prototype devices were designed and fabricated for proof-of-concept demonstration and for performing trade studies. The two devices were fabricated using off-the-shelf bellows with different spring rates. The properties of the two bellows are given in Table 1. The bellows were made of 304 stainless steel. The bellows were electron-beam welded to a base, in which electric cartridge heaters were embedded. A top end cap was also welded to the free end of the bellows. A layer of 100 mesh screen wick was tacked to the inner surface of the top and bottom end caps for improved condensation and evaporation processes, respectively. A test apparatus was constructed in which the bellows assembly was offset from a cold plate which could be held to a constant temperature. Thermocouples were mounted to the base of the device, along the length of the bellows, on the end cap, and on the heat sink to capture the temperature distribution. In addition to temperature measurements, the contact of the bellows with the heat sink was characterized by an electrical resistance measured across the test apparatus; a parallel shunt

resistor was used for finite resistance values, which were measured using a Keithley Sourcemeter 2450. An image of the test apparatus is given in Figure 3.

Table 1: Initial bellows selection for model validation

Bellows	Convolution ID cm (in)	Convolution OD cm (in)	Free Length cm (in)	Spring Rate - Vendor (N/m)	Spring Rate - Measured (N/m)
1	1.829 (0.72)	2.730 (1.075)	5.334 (2.1)	20140	20000
2	1.877 (0.739)	2.723 (1.072)	5.118 (2.015)	4203	~2200

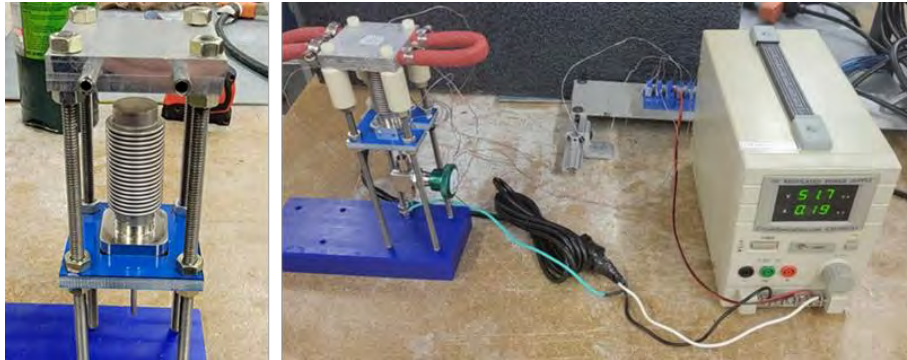


Figure 3: Two-phase thermal switch prototype test apparatus – vertical orientation in ambient

Testing was performed on the first thermal switch assembly in ambient pressure. The bellows was charged with 6 mL of acetone working fluid; enough to saturate the screen wicks and to fill the bellows convolutions, should the liquid get trapped there by capillary forces. Acetone was selected as the working fluid for this demonstration due to its ease of handling and testing temperatures. The heat sink interface was offset approximately 0.125 in (0.32 cm) from the natural length of the assembly. Several tests were performed with a constant heater power applied, while the sink temperature was reduced, from around 20 to 25°C to around -5 to 0°C. In these tests, the temperature of the cold plate was maintained by a single-phase water glycol mixture, which limited the minimum sink temperature. Measured temperature profiles and electrical resistance through the system are plotted in Figure 4(a) and (b) for input powers of 13.5 W and 20 W, respectively. As the sink temperature is reduced, the vapor temperature decreases slightly, but remains within a few degrees of its initial value. Correspondingly, the electrical resistance, which makes a step-change decrease when the bellows comes in contact with the sink, increases slightly, indicating that the bellows contact pressure is reduced as the vapor temperature decreases. This effect is seen more strongly in the 13.5 W test. However, intermittent contact of the bellows with the heat sink was not seen in the electrical resistance measurements.

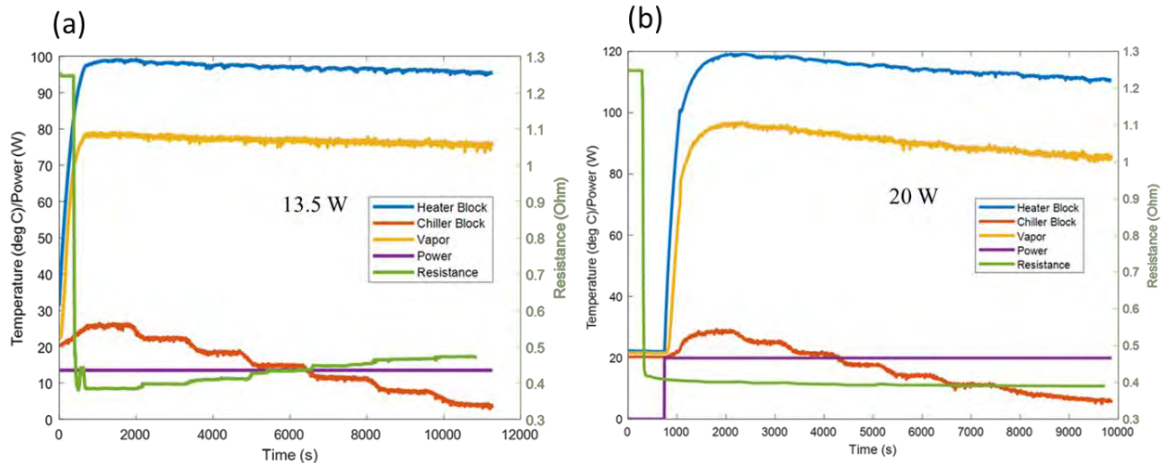


Figure 4: Constant power, variable sink test of first thermal switch assembly. Tested with acetone working fluid in ambient pressure. Input power of (a) 13.5 W and (b) 20 W.

Testing was performed on the second thermal switch assembly, this time in vacuum conditions at room temperature. Additionally, compared to the above testing of the above device, the testing was performed in a horizontal orientation with a slight gravity-aided tilt, as shown in Figure 5. Acetone was again used as the working fluid. In this test, a constant sink temperature of -40°C was maintained using liquid nitrogen. An initial power of 7 W was applied, and then stepped down to a minimum power of 0.8 W. The bellows contacted the heat sink around the setpoint temperature of 40°C , as indicated by the electrical resistance measurement. Once the power was dropped to 1 W, the bellows broke contact with the sink. To investigate hysteresis, the power was increased back to 2 W and then again dropped to 1 W. In each case, as the power is reduced to 1 W, the bellows goes into intermittent contact with the heat sink for roughly 100s, before fully detaching. This indicates that the heat leaks to the environment are on the order of 1 W. The measured temperature profile is shown in Figure 6, along with the input power (a) and measured electrical resistance (b).

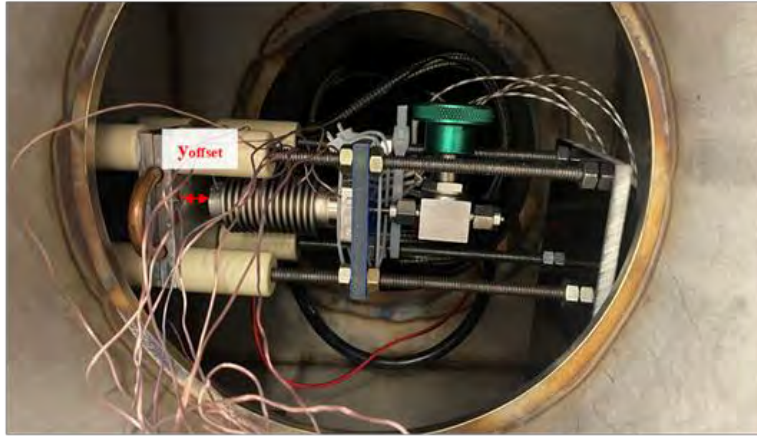


Figure 5: Two-phase thermal switch test apparatus - horizontal orientation in vacuum chamber

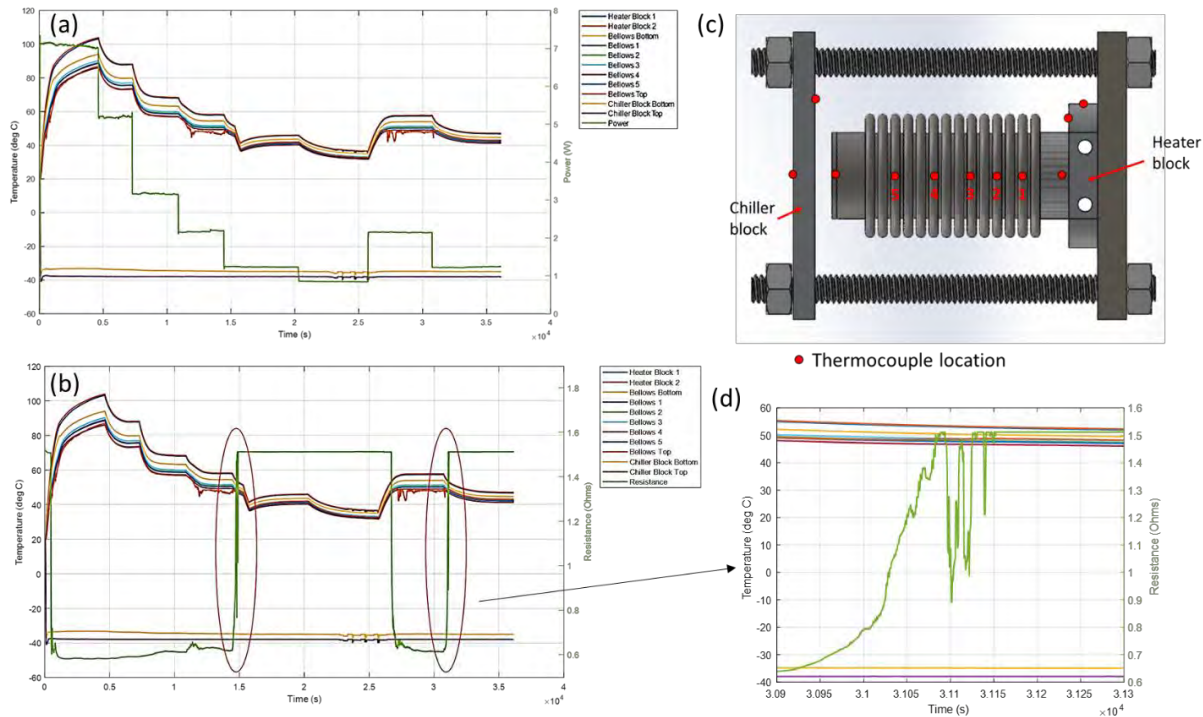


Figure 6: Constant sink test of second thermal switch prototype. Tested horizontally in vacuum with acetone working fluid. (a) Temperature distribution plotted with input power (b) Temperature distribution plotted with measured electrical resistance. Red ovals highlight intermittent bellows contact. (c) Bellows thermal switch thermocouple layout. (d) Detail of bellows oscillation

From the testing of these first thermal switch prototype devices, it is evident that the overall thermal resistance through the switch when “On” is dominated by the resistance at the interface between the bellows end cap and the heat sink. A model for the thermal resistance between two metal surfaces based on solid spot conductance can be used to estimate the thermal resistance of the interface. Inputs to this model include the modulus of elasticity, thermal conductivity, surface roughness and slope, and microhardness of the two surfaces (Ref. 4, 5). This model fairly accurately predicts the measured thermal interface resistance as a function of the acetone vapor pressure for reasonable values of the input parameters (1 μm surface roughness and 1560 MPa Al microhardness). There is some uncertainty about the values of these inputs, but the model still gives a reasonable approximation. From this analysis, it is reasonable to assume that the low vapor pressure of the acetone working fluid, and thus the low contact pressure at the interface, is a leading contributor to the interface thermal resistance, and that higher vapor pressure fluids would result in improved thermal resistance. However, it is worthwhile to look at other ways the interface could be further improved. Reducing the surface roughness by polishing the surface of the bellows end cap and the heat sink can improve the thermal resistance of the interface between the bare metal surfaces. Reducing the surface roughness from 1 μm to 0.2 μm can improve the thermal resistance by around 50%, based on the solid spot conductance model. Alternatively, a thermal interface material (TIM) may be used. The eGraf HITHERM 1205 thermal interface material was evaluated and the thermal interface resistance as a function of acetone vapor pressure was estimated from the material spec sheet, including the estimated resistance of an adhesive layer used to adhere the TIM to the bellows end cap. As shown in Figure 7, the compressible TIM can reduce the thermal interface resistance by roughly two orders of magnitude.

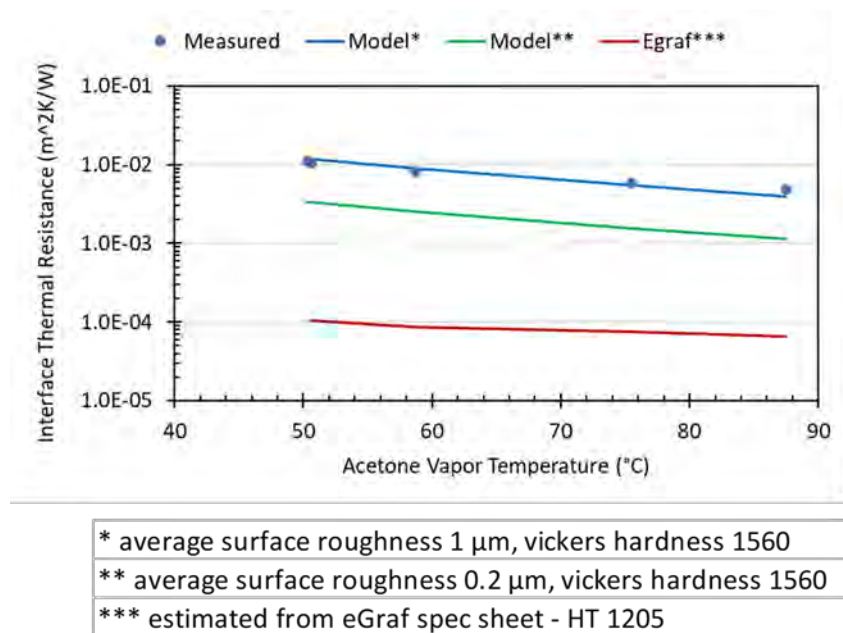


Figure 7: Estimated potential improvements in contact thermal resistance

To demonstrate the potential of the compressible TIM for improved thermal conductance, it was added to the surface of the second thermal switch prototype. Testing was performed to characterize the improvement. The working fluid was changed to methanol for this testing. Methanol has a similar vapor pressure to acetone, with a somewhat higher performance figure of merit. The tests were performed in a horizontal orientation, with a slight inclination for liquid return, in ambient pressure with a constant 20°C sink temperature, and varying input powers. Lower temperatures at the same powers and sink conditions while the bellows is fully in contact (i.e., the thermal switch is ON), indicated an increase in the ON conductance of the switch. Thermal conductances across the device as a whole and across the interface were calculated from the measured temperature distributions, and plotted in Figure 8. As can be seen, the conductance across the interface increases by around 1.5-1.7 \times .

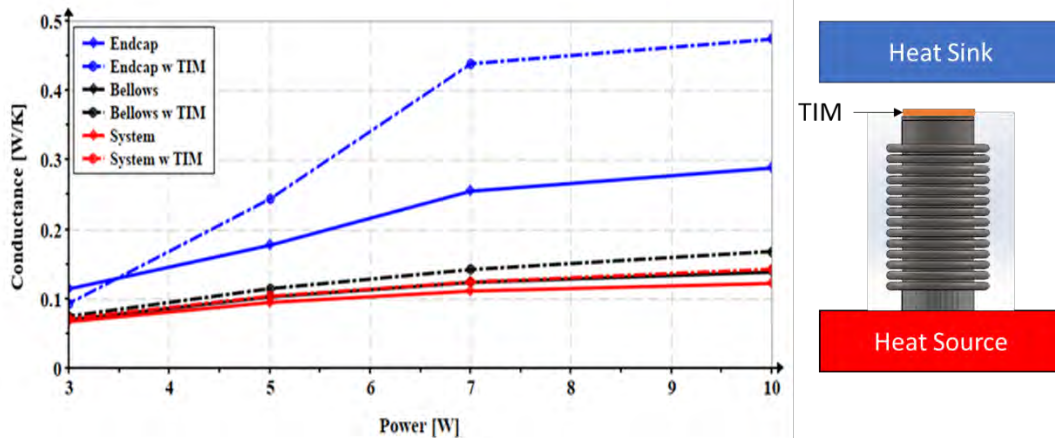


Figure 8: Comparison of thermal switch conductances with and without a compressible TIM. Interface, or “endcap” conductance increases by at least 1.5× with application of a TIM to bellows end cap surface.

IV. Thermal Switch Design for Small Lunar Rovers

One of the potential applications for the two-phase thermal switch is for enabling a high turndown ratio thermal management system for small lunar rovers. This class of rovers have masses on the order of a few kilogram, and heat dissipation requirements on the order of 10 W or less. Heat is rejected during the lunar day by a radiator that forms the top surface of the rover. The heat generating components may be mounted directly to the underside of the radiator. While this is effective for heat rejection during the lunar day, this configuration would not allow the rover to survive the lunar night.

ACT is developing a two-phase thermal switch based thermal management system for small rovers that would enable lunar night survival. This thermal management system concept is shown in Figure 9. In this concept, the current radiator panel/frame is converted to a heat collector plate or frame, to which the electronics are mounted in the same way as they would be to the bottom of the radiator. A new radiator panel is located above the heat collector plate and supported by low thermal conductivity standoffs. One or more two-phase thermal switches would be placed in the space between the heat collector plate and the radiator panel, with the bellows designed to come into contact with the radiator at a specified temperature corresponding to the minimum allowable temperature of the electronics. As an example, a contact temperature of -10°C is assumed. Based on this target contact temperature and expected operating temperature during the lunar day when the switch is ON, propylene is preliminarily selected as a working fluid for the bellows. The vapor pressure of propylene is used to select the bellows spring constant and radiator offset. The thermal switch is oriented to operate in a gravity-aided orientation (maximum tilt of the small lunar rover is $\pm 30^{\circ}$), thus a wick structure is not strictly required. However, a screen wick bridge may be included connecting the top and bottom internal bellows surface for improved liquid return.

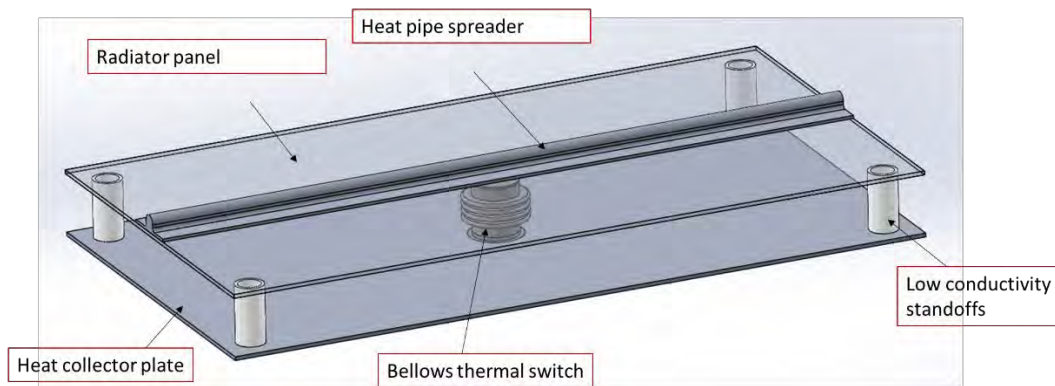


Figure 9: Thermal switch based thermal management system for small lunar rovers – conceptual schematic

A heat pipe is attached or embedded in the radiator, to both improve radiator efficiency through heat spreading, but also to provide structural support to prevent deflection of the radiator under the contact pressure of the bellows when operating in the ON condition during the lunar day. The heat pipe can utilize a screen wick to account for the potential 30° tilt of the rover. The total combined additional mass of the radiator, thermal switch assembly, and standoffs is estimated at roughly 0.5 kg.

A preliminary thermal analysis of this design concept was performed. In this case of polar noon, the lunar surface is estimated to have a surface temperature T_g of -50°C (223 K). Taking a worst-case scenario of a 30° tilt, the radiator would see the lunar surface with an estimated view factor of 0.067. Using the specified radiator area (10 cm × 20 cm) and emissivity (0.85), the radiator temperature can be estimated for a given heat load from the following equation:

$$Q_{rad} = \sigma \varepsilon A F_{A \rightarrow g} (T_A^4 - T_g^4) + \sigma \varepsilon A F_{A \rightarrow sky} (T_A^4 - T_{sky}^4) \quad (7)$$

For a total heat load of 7 W, the radiator temperature is estimated to be 20°C. Next, the vapor temperature within the bellows may be estimated based on the thermal switch thermal resistance network. Using an estimated order of magnitude contact resistance ($\sim 10^{-4}$ m²K/W), conduction through the end cap, and an estimated condensation heat transfer coefficient ($h = 7500$ W/m²K), the vapor temperature is estimated to be around 31°C. This is then used as a boundary condition for an finite element thermal simulation of the heat collector plate. Using an estimated evaporation heat transfer coefficient of 5000 W/m²K, the maximum temperature of the heat collector plate is found to be around 62°C. From this analysis, the overall estimated ON conductance for the thermal switch based thermal management system is on the order of 0.5 W/K. This ON conductance can be further increased through optimization of the bellows design and interfaces.

During the OFF condition for the thermal switch during the lunar night, the switch thermally decouples the heat collector plate and the radiator, enabling the rover electronics to be maintained above their minimum temperatures, while allowing the radiator to reach low temperatures. Thus, it is essential to minimize heat leak paths from the heat collector plate to the radiator. Layers of MLI can be placed in the space between heat collector plate and the radiator to minimize radiative losses. The primary heat leak path is then through the radiator standoffs. By clever design of these standoffs and utilizing low thermal conductivity materials such as PEI (Ultem), an OFF conductance G_{off} on the order of $10^{-4} - 10^{-3}$ W/K can be achieved. A quick analysis can determine the effect of the OFF conductance on survival heater power required to maintain electronics above their minimum survival temperature. If it is desired to maintain the heat collector plate temperature at the minimum survival temperature of -20°C, the heat leak through thermal switch system (i.e., the required survival power) can be estimated from the following equations:

$$Q_{rad} = \sigma \varepsilon A F_{rad \rightarrow g} (T_{rad}^4 - T_g^4) + \sigma \varepsilon A F_{rad \rightarrow sky} (T_{rad}^4 - T_{sky}^4) \quad (8)$$

$$Q_{rad} = G_{off} (T_{plate} - T_{rad}) \quad (9)$$

For the same radiator configuration as previous, the heat leaks to maintain the plate at 253 K and resulting radiator temperatures are given in Table 2 for the full range of estimated Off conductances.

Table 2: Estimated heat leaks/survival power and resulting radiator temperature to maintain collector plate at minimum survival temperature during lunar night

Off Conductance (W/K)	Heat Leaks (W)	Radiator Temperature (K)	On/Off Conductance Ratio
10^{-4}	0.014	67	~4500
10^{-3}	0.186	110	~450

A prototype thermal switch based thermal management system for small rover lunar night survival is currently being designed and fabricated for testing.

V. Conclusions

A two-phase thermal switch is under development for lunar lander and rover thermal management applications. This thermal switch concept utilizes the vapor pressure of a saturated working fluid to passively actuate the switch at a specified set point temperature. Proper design of the thermal switch can enable the high thermal turndown ratios needed for lunar night survival, while also effectively rejecting waste heat during the lunar day.

A coupled thermal-mechanical model was developed for investigating the dynamic behavior of the thermal switch. Two proof-of-concept two-phase thermal switch devices were fabricated and tested under a range of conditions. Testing under constant power-variable sink and constant sink-variable power conditions, both in ambient and in vacuum, and both horizontally and vertically, showed expected behavior. Testing indicated that the contact interface between the bellows and the heat sink is critical to overall thermal resistance, and improvement in thermal resistance from the use of a compressible thermal interface material was demonstrated.

Finally, a design concept for a two-phase thermal switch based thermal management system for small lunar rovers to enable lunar night survival was presented. Preliminary thermal analysis of the design concept demonstrated its feasibility. A prototype thermal switch for small lunar rovers is currently being developed for an experimental demonstration of the concept.

Acknowledgments

This project is sponsored by NASA Marshall Space Flight Center under SBIR Sequential Phase II Contract No. 80NSSC21C0614. ACT would like to thank our technical monitor Jeff Farmer.

Additionally, ACT acknowledges the support of Braden Flinchbaugh and Jonathan Murray, the technicians who supported the prototype fabrication and testing at ACT.

References

¹Sunada, E., Pauken, M., Novak, K., Phillips, C., Birur, G., and Lankford, K., "Design and Flight Qualification of a Paraffin-Actuated Heat Switch for Mars Surface Applications." SAE Technical Paper No. 2002-01-2275, 2002.

²Marland, B., Bugby, D., Stouffer, C., Tomlinson, B., and Davis, T., "Development and Testing of a High Performance Cryogenic Thermal Switch." *Cryocoolers 11*, edited by R. G. Ross, Springer US., 2002. pp. 729-738.

³Bugby, D.C., and Rivera, J.G., "High Performance Thermal Switch for Lunar and Planetary Surface Extreme Environments." International Conference on Environmental Systems, 2020

⁴Lambert, M.A., and Fletcher, L.S., "Review of Models for Thermal Contact Conductance of Metals." *Journal of Thermophysics and Heat Transfer*, 11(2), 129-139, 1997.

⁵Bahrami, M., Culham, J.R., Yovanovich, M.M., "Modeling Thermal Contact Resistance: A Scale Analysis Approach." *Journal of Heat Transfer*, 126, 896-905, 2004.